A TURBULENT IMMERSED AIR WALL JET ON A BURNING GRAPHITE SURFACE

É. P. Volchkov and P. V. Nikitin

The turbulent boundary layer in an immersed air jet traveling along a burning graphite wall is analyzed. In order to study the heat and mass transfer and the friction in the boundary layer, a method of calculation based on the solution of the integrated energy and momentum relations is employed, allowing for the conservative properties of the turbulent boundary layer at the wall [1].

NOTATION

x – longitudinal coordinate
y – transverse coordinate
s – height of slot
δ – thickness of boundary layer
δ^* – displacement thickness
δ^{**} – momentum-loss thickness,
ω – velocity
j – transverse mass flow (flux)
ρ – density
T – temperature
i – total enthalpy
ψ – temperature factor
ψ_1 – enthalpy factor
k – reduced concentration of the i-th component
τ – tangential stress
b – permeability parameter
C_1 – form (shape) parameter
μ – dynamic viscosity coefficient
c_f – friction coefficient
Ψ – relative friction coefficient

INDICES

w – parameters at the wall; 0 – parameters at the outer boundary of the boundary layer; ∞ – parameters outside the wall; s – parameters in the slit (slot).

1. Integrated Characteristics of the Boundary Layer at the Wall. Let us consider a turbulent stream of gas flowing out of a slot and traveling along the surface (Fig. 1). Gas is drawn in from the surrounding space and moves with the gas jet. The surface around which the gas is flowing may enter into chemical reactions with the gas flow, as a result of which a transverse flow of matter $j_W = \rho_W w_W$ is created at the wall. At the wall a "wall" boundary layer δ thick develops. At the outer boundary of this layer the velocity takes its maximum value in this section: $\partial w_x/\partial y = 0$.

Let us integrate the equation of motion of the boundary layer along the y axis from y = 0 to y = δ

$$\rho w_x \frac{\partial w_x}{\partial x} + \rho w_y \frac{\partial w_x}{\partial y} = \frac{\partial \tau}{\partial y} \tag{1.1}$$

allowing for the continuity equation

$$\frac{\partial \rho w_x}{\partial x} + \frac{\partial \rho w_y}{\partial y} = 0 \tag{1.2}$$

Novosibirsk. Translated from Zhurnal Prikladnoi Mekhaniki i Tekhnicheskoi Fiziki, No. 1, pp. 60-67, January-February, 1971. Original article submitted March 3, 1970.

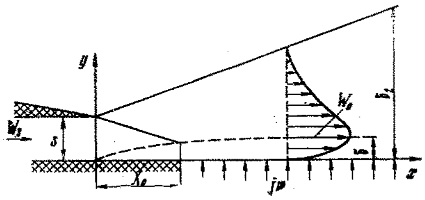

Fig. 1

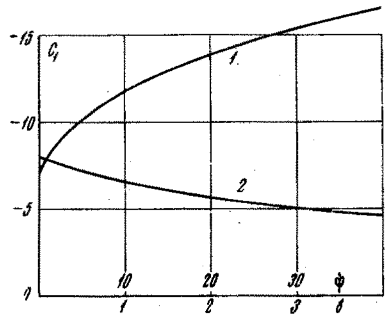

Fig. 2

and the boundary conditions for the layer under consideration

$$\begin{aligned} &\tau = \tau_w, \quad w_x = 0, \quad \rho w_y = j_w \quad (y = 0) \\ &\tau = 0, \quad w_x = w_0 = f(x) \quad (y = \delta) \end{aligned} \tag{1.3}$$

As a result of this we obtain the integrated momentum equation of the boundary layer at a permeable wall in an immersed jet:

$$\frac{dR^{**}}{dX} + \left(1 + \frac{\delta^*}{\delta^{**}} - \frac{\delta}{\delta^{**}}\right)\frac{R^{**}}{W_0}\frac{dW_0}{dX} = \frac{c_{f_1}}{2}(1 + b_1) R_s W_0 \tag{1.4}$$

$$W_0 = \frac{w_0}{w_s}, \quad X = \frac{x}{s}, \quad c_{f_1} = \frac{2\tau_w}{\rho_0 w_0^2} \tag{1.5}$$

$$\delta^* = \int_0^\delta \left(1 - \frac{\rho w}{\rho_0 w_0}\right) dy, \quad \delta^{**} = \int_0^\delta \frac{\rho w}{\rho_0 w_0}\left(1 - \frac{w}{w_0}\right) dy, \quad b_1 = \frac{j_w 2}{\rho_0 w_0 C_{f_1}} \tag{1.6}$$

Here δ^*, δ^{**} are the displacement thickness and the momentum-loss thickness of the boundary layer, respectively; c_{f_1} is the local coefficient of friction calculated from the maximum velocity in the cross section under consideration, and b_1 is the permeability parameter of the wall.

The viscosity of the gas at the outer boundary of the wall boundary layer may, in general, vary. In the integration equation (1.4), however, on transforming to dimensionless quantities it is convenient to use a constant viscosity value, since this enters under the sign of the differential. In the case under consideration we therefore used the viscosity of the gas in the slot. The Reynolds numbers based on the momentum-loss thickness and slot, respectively, may accordingly be defined thus:

$$R^{**} = \frac{\rho_0 w_0 \delta^{**}}{\mu_s}, \quad R_s = \frac{\rho_s w_s s}{\mu_s}$$

For brevity we may write

$$C_1 = 1 + \frac{\delta^*}{\delta^{**}} - \frac{\delta}{\delta^{**}} \tag{1.7}$$

In order to solve the integrated relationship (1.4) we require the law governing the change in the maximum velocity with length, the law of friction, the permeability factor b_1, and the form parameter C_1.

1. In an immersed flat jet propagating in a space filled with gas of the same density ($\rho_s = \rho_\infty$) the maximum velocity varies in accordance with a power law [1, 2]

$$W_0 = C_2 X^a \tag{1.8}$$

2. We take the law of friction in the wall boundary layer in the form [3, 4]

$$\frac{c_{f_1}}{2} = AR^{**-m}\left(\frac{\mu_w}{\mu_s}\right)^m \Psi, \quad \Psi = \left(\frac{c_{f_1}}{c_{f_0}}\right)_{R^{**}} = \left(\frac{S_1}{S_0}\right)_{R^{**}_T} \tag{1.9}$$

Here μ_w is the dynamic viscosity at the wall, Ψ is the relative law of heat and mass transfer and friction; for developed turbulent flow [3], with $R^{**} < 10^4$, we have $A = 0.0128$, $m = 0.25$.

In a uniform, subsonic boundary layer, when the wall temperature is greater than the temperature of the circumfluent gas ($\Psi_1 > 1$), the limiting relative law may be used [3]

$$\Psi = \frac{4}{b_1(\psi_1 - 1)}\left\{\operatorname{arc\,tg}\left[\frac{b_1}{(\psi_1 - 1)(b_1 + 1)}\right]^{1/2} - \operatorname{arc\,tg}\left[\frac{b_1\psi_1}{\psi_1 - 1}\right]^{1/2}\right\}^2 \left(\psi_1 = \frac{i_w}{i_0}\right) \tag{1.10}$$

Here i_W and i_0 are the total enthalpies of the gas at the wall and at the outer boundary of the wall boundary layer.

3. If the chemical reactions at the wall take place in the diffusion mode (in which the process is determined by the rate of diffusion and not by the velocity of the chemical reaction), the permeability parameter b_1 may be expressed in terms of the reduced weight concentrations of the chemical elements entering into the reaction [5, 6]. The reduced concentration is the concentration of the chemical element, independently of the state in which it occurs (free or in a chemical compound).

In the case of the interaction of graphite with the oxygen in a gas stream, which leads to the reaction

$$C + 0 \rightarrow CO \tag{1.11}$$

at the wall ($T_W \geq 1500°K$), the permeability parameter is determined [5, 6] from the reduced concentrations of the oxidizing agent K(0) and the reduced concentrations of the carbon K(C)

$$b_1 = \frac{K(0)_0}{K(0)_w} - 1, \quad \frac{b_1}{1 + b_1} = K(C)_w \tag{1.12}$$

For the diffusion mode of combustion, when the reaction (1.11) takes place at the wall, we have

$$K(C)_w = {}^{12}/_{28}K(CO)_w, \quad K(0)_w = {}^{16}/_{28}K(CO)_w \tag{1.13}$$

Finally, from Eqs. (1.12) and (1.13) we obtain an expression for the permeability parameter

$$b_1 = \frac{K(C)_w}{K(0)_w}K(0)_0 = \frac{3}{4}K(0)_0 \tag{1.14}$$

Equation (1.14) is obtained subject to the condition of similarity between the heat-and-mass-transfer and friction processes, i.e., $\frac{1}{2}c_{f_1} = S_1$. Thus, for a stream of air propagating in a space filled with air, $K(0)_0 = 0.232$,

$$b_1 = \frac{j_w}{\rho_0 w_0 S_1} = \frac{j_w}{\rho_0 w_0}\frac{2}{c_{f_1}} = 0.173, \quad S_1 = \frac{j_w}{\rho_0 w_0 b_1} \tag{1.15}$$

Here S_1 is the Stanton diffusion number, calculated from the velocity at the outer boundary of the wall boundary layer.

4. It was shown in [1] that, when gas flowed around an impermeable wall under isothermal conditions, the form parameter $C_1 = -8$. Let us find how the existence of nonisothermal conditions and permeability of the wall affect C_1. For this purpose we shall analyze the changes taking place in the integrated characteristics of the boundary layer

$$\frac{\delta^*}{\delta} = \int_0^1\left(1 - \frac{\rho}{\rho_0}\omega\right)d\eta, \quad \frac{\delta^{**}}{\delta} = \int_0^1 \frac{\rho}{\rho_0}\omega(1 - \omega)\,d\eta \tag{1.16}$$

Here $\omega = w_x/w_0$, $\eta = y/\delta$.

The density distribution over the cross section of the boundary layer may be found from the equation of state of an ideal gas, and from the condition of similarity between the velocity and temperature profiles in the wall boundary layer [3]

$$\frac{\rho_0}{\rho} = \psi + (1 - \psi)\,\omega, \quad \psi = \frac{T_w}{T_0} \tag{1.17}$$

Taking $\omega = \eta^{1/7}$ and integrating Eq. (1.16), allowing for (1.17), we have

$$\frac{\delta^*}{\delta} = 1 - 7\left[\frac{\psi^7}{(1-\psi)^8}\ln\psi + \sum_{\nu=0}^{6}\frac{(-1)^\nu\psi^\nu}{(7-\nu)(1-\psi)^{\nu+1}}\right] \tag{1.18}$$

$$\frac{\delta^{**}}{\delta} = 7\left[\frac{\psi^7}{(1-\psi)^8}\ln\psi + \frac{\psi^7}{(1-\psi)^8} + \sum_{\nu=0}^{6}\frac{(-1)^\nu\psi^\nu}{(7-\nu)(8-\nu)(1-\psi)^{\nu+1}}\right] \tag{1.19}$$

In order to analyze the influence of mass transfer at the impermeable wall on the integrated characteristics of the boundary layer, we make use of the velocity profile obtained for this case in [7], with ρ = const

$$\omega = 1 - \sqrt{\Psi + b}\,(1-\omega_0) + {}^1/_4 b\,(1-\omega_0)^2 \tag{1.20}$$

Here $\omega_0 = \eta^{1/7}$ is the velocity distribution in an isothermal boundary layer at an impermeable plate. In this case the relative law of mass-and-heat transfer and friction [7] is

$$\Psi = (1 - {}^1/_4 b)^2, \quad b = b_1\Psi = \frac{j_w}{\rho_0 w_0}\,\frac{2}{c_{f_0}} \tag{1.21}$$

Then from Eqs. (1.16) and (1.20) we find the dependence of the integrated characteristics of the boundary layer on the inflow

$$\frac{\delta^*}{\delta} = \frac{1}{8}\left(\sqrt{\Psi + b} - \frac{b}{18}\right) \tag{1.22}$$

$$\frac{\delta^{**}}{\delta} = \frac{1}{8}\left(\sqrt{\Psi + b} - \frac{b}{18}\right) - \frac{1}{36}(\Psi + b) + \frac{1}{240}\sqrt{\Psi + b} - \frac{b^2}{5280} \tag{1.23}$$

In Fig. 2, curve 1 represents the dependence of the form parameter C_1 on the nonisothermal factor (for b = 0) and on the inflow (or blast) (for $\psi = 1$); curve 2 is calculated from Eqs. (1.16)-(1.23).

Together with the law of friction (1.9), the integrated momentum relation (1.4) gives a linear differential equation.

In general form, the solution of this is

$$R^{**} = W_0^{-C_1}\left[A(m+1)R_s\int_{X_0}^{X} W_0^{C_1(m+1)+1}(1+b_1)\Psi\left(\frac{\mu_w}{\mu_s}\right)^m dX + (R^{**}W_0^{C_1})_{X_0}^{1+m}\right]^{(1+m)^{-1}} \tag{1.24}$$

For b = const, and with a constant wall temperature, Ψ = const. In the main region of the flow ($X \gg X_0$) we then obtain the following from Eq. (1.24) with due allowance for (1.8):

$$R^{**} = \left[\frac{A(m+1)R_s\Psi(1+b_1)C_2X^{a+1}}{aC_1(m+1)+a+1}\left(\frac{\mu_w}{\mu_s}\right)^m\right]^{(m+1)^{-1}} \tag{1.25}$$

Let us substitute Eq. (1.25) into the law of friction (1.9); using the relation $S_1 = \frac{1}{2}c_{f_1}P^{-0.6}$ we finally obtain:

$$S_1 = \frac{A\Psi[aC_1(m+1)+a+1]^n}{[A(m+1)R_s\Psi(1+b_1)C_2X^{a+1}]^n P^{0.6}}\left(\frac{\mu_w}{\mu_s}\right)^n, \quad n = \frac{m}{m+1} \tag{1.26}$$

For practical calculations it is more convenient to use the Stanton number, which is determined from the parameters in the slot. In this case,

$$S_2 = \frac{j_w}{\rho_s w_s b_1} = S_1 W_0 = S_1 C_2 X^a \tag{1.27}$$

2. Experimental Investigation. Experiments were carried out in an apparatus providing for the inductive heating of a graphite channel. A complete description of the apparatus was given in [5]. The arrangement of the working part in which the experiments were conducted is shown in Fig. 3. As working parts we used cylindrical samples 1 with an internal diameter of 41 mm, an external diameter of 60 mm, and a length of 190 mm. The samples were made of graphite with a density of $\gamma = 1895$ kg/m^3.

An air jet was passed into the channel through an annular tangential slot s = 2.08 mm wide formed by two coaxial nozzles 2 and 3. From the surrounding space air was drawn into the chamber through the inner nozzle 3. The gas from the channel was expelled into the atmosphere. The flow of air passing into the slot was measured by means of flowmeters. The temperature of the air remained practically the same in all the experiments: $T_S = T_\infty \approx 290$°K.

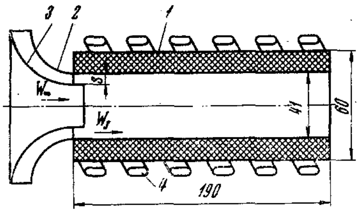

Fig. 3

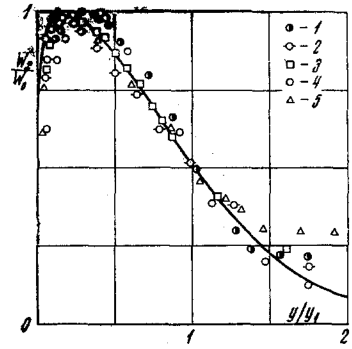

Fig. 4

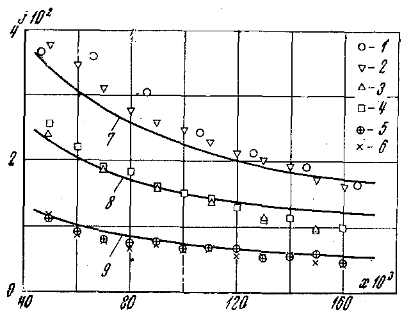

Fig. 5

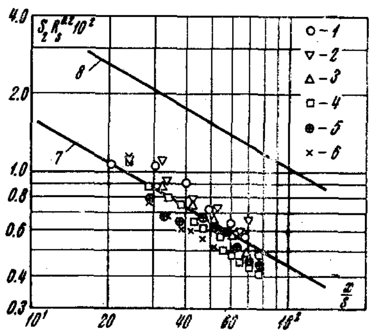

Fig. 6

First we made a number of calibration experiments under isothermal conditions in the absence of chemical reactions at the wall. The aim of these experiments was that of obtaining the characteristics of the wall jet and comparing with existing data. In the experiments the Reynolds number with respect to the slot R_s varied from $3.6 \cdot 10^3$ to $17 \cdot 10^3$, which corresponded to a change in velocity w_s from 26.2 to 124 m/sec. As a result of the ejection of air from the surrounding space the relative velocity was $w_s/w_\infty = 3.8$-4.

The velocity profiles of the jet were measured under isothermal conditions by means of a total-head tube. The tube had an elliptical cross section 0.25 mm high and 1 mm broad. This was introduced into the channel through a groove 10 mm wide. The measurements were made at the opposite wall. The tube was moved in the vertical and horizontal directions by means of a locating system with a scale division of 0.05 mm.

We shall now give the results of the measurements and also present a comparison with experiments on a wall jet at a flat plate [2]. In Fig. 4, the curve represents the Glauert velocity profile [8] in a wall jet; the points 1, 2, and 3 (measurements in the tube) and points 4 and 5 of [2] (measurements at a plate) correspond to the following parameters:

Points	1	2	3	4	5	
$X =$	11.3	56.9	32.7	9.6	73	
$w_s =$	26.2	48.8	124	30.2	64.4	m/sec
$W_0 =$	28.5	31	93	32.6	28.7	
$y_1 =$	3.3	10.5	6.8	2.16	10.9	mm

We see that the velocity profiles of the wall jet obtained in the present investigation for flow in a tube ($s/D_0 = 0.0508$) are in excellent agreement with the velocity profiles in a plane jet [2, 8]. The transverse coordinate y_1 in Fig. 4 corresponds to the point at which the velocity equals half the maximum value in the section under consideration.

The experimental results obtained by measuring the maximum velocity of the wall jet in the tube closely follow the relation

$$W_0 = 3.6\, X^{-0.45} \qquad (2.1)$$

obtained in [2] for plane flow over a relative inflow velocity range of $3 < w_s/w_\infty < 9$. Evidently in the present case (for $s/D_0 = 0.0508$ and $x/D_0 \leq 5$) the transverse curvature has no serious effect on the characteristics of the wall jet, and the flow in this is similar to that of a plane jet.

We also studied the heat and mass transfer in a wall air jet at the burning surface of a cylindrical graphite channel. In this case the graphite sample 1 (Fig. 3) was heated to T_W = 1900-2000°K by means of an inductor 4 attached to a high-frequency generator. This corresponded to a slight change in the enthalpy factor $8.3 \leq \psi_1 \leq 8.7$. The temperature of the graphite wall was measured with an OPPIR-017 optical pyrometer. The nonuniformity in the temperature distribution along the wall (from 30 to 170 mm) was no greater than 6%. For a wall temperature of T_W > 1500°K reaction (1.11) passed into the diffusion mode. During the heating of the graphite channel to the working temperature, and also during the cooling period at the end of the experiment, an inert gas (nitrogen or argon) was passed through the slot into the channel, and the inner nozzle 3 was tightly closed with a shaped stopper. This was done to eliminate the possible combustion of the surface while heating and cooling. When the sample had been heated to the required temperature, the stopper was taken away from the nozzle 3 and air was passed into the slot instead of the inert gas.

During the experiment (τ = 80-200 sec), a 1-2 mm thickness of graphite was carried away. After the experiment the sample was cut into cylindrical sections 10 mm wide. The thickness of combustion was determined by measuring the initial and final internal diameters. The final internal diameter was measured on a comparator with a scale division of 1 μ.

The mass flow of material in the wall was determined from the relation

$$j_w = \frac{\delta\gamma}{\tau} = \frac{(D^* - D_0)\gamma}{2\tau} \tag{2.2}$$

Here δ is the thickness of the burned layer of graphite, γ is the density of the graphite, τ is the burning time, D^* is the final diameter, and D_0 is the initial diameter.

The experimental values of the Stanton criterion were calculated from the equation

$$S_2 = \frac{j_w}{\rho_s w_s b_1} \tag{2.3}$$

where the value of the parameter b_1 was determined from (1.15).

In order to carry out a calculation on the basis of Eqs. (1.26) and (1.27) we must know the law of variation of the maximum velocity and the value of the form parameter C_1. Under the conditions of the experiments, the permeability parameter was small: $b = b_1\Psi < 0.1$. The value of $C_1 \approx -11$ is determined from Fig. 2 as a function of the nonisothermal parameter ψ only. Then, using this value of C_1 and the law of variation of the maximum velocity (2.1), we obtain from Eqs. (1.26) and (1.27):

$$S_2 R_s^{0.2} = \frac{0.12}{X^{0.56} p^{0.6}} \left(\frac{\mu_w}{\mu_s}\right)^{0.2} \Psi^{0.8} \tag{2.4}$$

In this case, Ψ is determined from Eq. (1.10), and it is assumed that the Prandtl and Schmidt numbers are equal. Figure 5 shows the intensity of combustion $j_W 10^2$ (kg/sec · m²) of the graphite along the length of the channel $x10^3$ (m) in an immersed wall jet of air for three different velocities in the slot. Two experiments were made in each mode. The points 1, 2, 3, 4, 5, 6 correspond to the following values of the parameters:

Points	1	2	3	4	5	6
$w_s =$	114	113.4	59.6	72.7	27.4	25.95
$T_w =$	1923	1928	1938	1988	1997	1959

Curves 7, 8, 9 in Fig. 5 are calculated from the equation

$$j_w = \frac{0.12 b_1 \rho_s w_s \Psi^{0.8}}{X^{0.56} R_s^{0.2} p^{0.6}} \left(\frac{\mu_w}{\mu_s}\right)^{0.2} \tag{2.5}$$

for velocities in the slot of, respectively, 114, 66, and 26.7 m/sec.

The same experimental data are presented in Fig. 6. We see that on analyzing the data in this way the results correlate excellently. The notation of the experimental points 1, 2, 3, 4, 5, 6 is the same as in

Fig. 5. The continuous line 7 is based on a calculation by Eq. (2.4) with $\psi_1 = 8.5$. For comparison we also show the calculated curve 8 under isothermal conditions with $\psi_1 = 1$. We see that the departure from isothermal conditions in the present case reduces the intensity of mass and heat transfer by more than a factor of two by comparison with isothermal circumfluence.

LITERATURE CITED

1. É. P. Volchkov, S. S. Kutateladze, and A. I. Leont'ev, "Interaction of an immersed turbulent jet with a solid wall," Zh. Prikl. Mekhan. i Tekh. Fiz., No. 2 (1965).
2. R. A. Seban and L. H. Back, "Velocity and temperature profiles in a wall jet," Internat. J. Heat and Mass Trans., 3, No. 4 (1961).
3. S. S. Kutaladze and A. I. Leont'ev, Turbulent Boundary Layer of Compressible Gas [in Russian], Izd. SO AN SSSR, Novosibirsk (1962).
4. A. I. Leont'ev and B. P. Mironov, "Extension of the limiting relative laws of friction and mass transfer to the nonisothermal flow of gas with finite Reynolds numbers," Zh. Prikl. Mekhan. i Tekh. Fiz., No. 5 (1965).
5. A. I. Leont'ev, É. P. Volchkov, E. G. Zaulichnyi, and E. I. Sinaiko, "Experimental determination of the rate of loss of graphite under very nonisothermal conditions," Fiz. Goreniya i Vzryva, No. 2 (1967).
6. Lies, "Convective heat transfer in the presence of an inflow of material and chemical reactions," in: Gas Dynamics and Heat Transfer in the Presence of Chemical Reactions [Russian translation], IL, Moscow (1962).
7. Wall Turbulence [in Russian], Izd. SO AN SSSR, Novosibirsk (1968).
8. M. Glauert, "The wall jet," J. Fluid Mech., 1, No. 6 (1956).